



Structure and Properties of Hot-Pressed $\text{Pb}(\text{Lu}_{1/2}\text{Nb}_{1/2})\text{O}_3$ - PbTiO_3 Binary System Ceramics*

M. ANTONOVA, L. SHEBANOVS, M. LIVINSH, J.Y. YAMASHITA,¹ A. STERNBERG, I. SHORUBALKO & A. SPULE

Institute of Solid State Physics University of Latvia, LV-1063 Riga, Latvia

¹*Materials and Research Laboratories, Yanagi-Cho Works 18-2F, Toshiba Corporation, 70 Yanagi-Cho, Saiwai-ku, Kawasaki-city 210-8501, Japan*

Submitted May 4, 1999; Revised August 18, 1999; Accepted August 23, 1999

Abstract. Solid solution series of the $(1-x)\text{Pb}(\text{Lu}_{1/2}\text{Nb}_{1/2})\text{O}_3 - x \text{PbTiO}_3$ binary system ceramics (PLuNT) were synthesized and hot-pressed (temperature 950°C to 1130°C, pressure 25 MPa); its structure, dielectric and piezoelectric properties were studied. Pure lutecium niobate PLuN ($x = 0$) has a pronounced long-range order in the B-sublattice and an antiferroelectric to paraelectric phase transition at $\sim 258^\circ\text{C}$. The phase structure of the PLuNT system, at room temperature, changes from a pseudomonoclinic (psd-M, space group Bmm2) to tetragonal (T, space group P4mm). The pseudomonoclinic phase extends over the $0 \leq x \leq 0.38$ interval within which the monoclinic angle β proceeds a minimum near to 90° at $x \cong 0.2$. The morphotropic region covers the interval $x = 0.38 - 0.49$, the concentration ratio psd-M:T $\cong 1$ (the morphotropic phase boundary—MPB) corresponds to $x = 0.41$. Within the morphotropic region, a rather strong distortion of the unit cell— $(c/a - 1) \geq 0.02$, $\beta \geq 90.37^\circ$, characteristic of “hard” piezoelectrics is maintained. Dielectric dispersion and broadening of the phase transition, features typical to relaxors, are observed within the concentration interval of $0.1 \leq x \leq 0.3$. The highest electromechanical coupling coefficients: $k_p = 0.66$, $k_t = 0.48$, $k_{31} = 0.34$ of $(1-x)$ PLuN - x PT ceramics are attained in compositions near the MPB at $x \approx 0.41$. Non-isovalent doping of PLuNT with La^{3+} in Pb sublattice shifts the MPB to lower values of x .

Keywords: binary systems, lutecium niobate, relaxor, phase diagram, dielectric and electromechanical properties

1. Introduction

Recently much attention has been paid to electro-mechanical (piezoelectric, electrostrictive) materials because of their promising application in electronics, ultrasound transduction, acoustic sensing, microelectromechanical systems (MEMS). Substitutions of other cations in A and B sites of the piezoelectric perovskite $\text{Pb}(\text{Zr,Ti})\text{O}_3$ (PZT) [1] (compositions near morphotropic phase boundary (MPB), which divides the rhombohedral (R) and tetragonal (T) phases) have been used to optimise and to improve the electro-

mechanical (EM) properties of these materials. An alternative approach is to create complex perovskites—binary, ternary and many-component systems, including $\text{Pb}(\text{B}', \text{B}'')\text{O}_3$ compounds, mainly relaxors, and lead titanate PbTiO_3 (PT). Important reported systems include: $[\text{Pb}(\text{Mg}_{1/3} \text{Nb}_{2/3})\text{O}_3$ (PMN)-PT] (PMNT) [2,3], $[\text{Pb}(\text{Sc}_{1/2} \text{Nb}_{1/2})\text{O}_3$ (PSN)-PT] (PSNT) [4–6], $[\text{Pb}(\text{Sc}_{1/2} \text{Ta}_{1/2})\text{O}_3$ -PT] [7], [PSN-PMN-PT] (PSMNT) [8], PMN-PSN and $[\text{Pb}(\text{Zn}_{1/3} \text{Nb}_{2/3})\text{O}_3$ (PZN)-PSN] [9], PZN-PMN-PT [10], $\text{Pb}(\text{Yb}_{1/2} \text{Nb}_{1/2})\text{O}_3$ -PT [11], $\text{Pb}(\text{In}_{1/2}\text{Nb}_{1/2})\text{O}_3$ -PT [12] and $[\text{Pb}(\text{Ni}_{1/3}\text{Nb}_{2/3})\text{O}_3$ (PNN)-PT-PZ] [13]. Strong EM coupling ($k_p = 0.76$, $k_t = 0.56$, $k_{31} = 0.46$, $k_{33} = 0.79$) has been reported by T. Yamamoto [14] in hot-pressed PSNT ceramic samples

*The authors are grateful to Dr. K. Hayashi of Hayashi Chemical Ltd., Kyoto, Japan for financial support.

with grain size $\sim 1 \mu\text{m}$ and by Y. Yamashita [8] in PSMNT ternary ceramic material— $k_p = 0.72$, $k_{31} = 0.45$, $k_{33} = 0.77$, the piezoelectric coefficient d_{33} reaching 640 pC/N. The value of $d_{33} \approx 815$ pC/N is reported by Tai-Bor Wu [15] in 5 mol% La modified PMNT ceramics, the maximum value of k_{33} in ceramics up to 0.8 and $d_{33} = 900$ pC/N were attained in the 0.5PNN-0.345PT-0.155PZ composition [13].

A large effective piezoelectric coefficient $d_{33} \approx 1800$ pC/N, unusual in ceramics, has been achieved by J. Zhao [16] in the electric field induced state of PMNT (~ 0.2 PT) compositions (bias field 2.5 kV/cm, $T = 80^\circ\text{C}$); the strain at 10 kV/cm—0.15% (in composition near 0.3 PT).

Furthermore, an essential advantage compared to conventional PZT compositions is the considerable ease of growing some of the above complex perovskite single crystals [17–19]. Large values of k_{33} and d_{33} have been reported in single crystals— $k_{33} \approx 0.92$ in PZNT [17], $d_{33} = 1500$ pC/N in PMNT [20]. Park and ShROUT have observed ultrahigh strain levels of up to 1.7% (under electrical bias 120 kV/cm) and $k_{33} > 0.9$, $d_{33} \geq 2000$ pC/N in PZNT ($x = 0.08\text{PT}$) crystals grown by the flux technique [19].

Consequently, new complex perovskites are of interest to be introduced, and from such a viewpoint lead lutecium niobate ($\text{Pb}(\text{Lu}_{1/2}\text{Nb}_{1/2})\text{O}_3$ (PLuN)-PT) binary system (further abbreviated as PLuNT) was studied in this work for the first time with the purpose of high temperature application.

The phase diagrams of ferroelectric two (multi)-component perovskite solid solutions often contain the morphotropic region where, due to the change of concentration of one of the components, sharp transitions between non-equivalent crystallographic structures occur regardless of the temperature.

Compositions close to the MPB or within the morphotropic region have excellent piezoelectric properties. Polarization of ceramics in the morphotropic region proceeds more easily because: (1) the values of spontaneous deformation, e.g., in case of PZT, $(c/a - 1)$ of the tetragonal P4mm phase, $\cos \alpha$ of the rhombohedral R3m phase—are small making the material liable to different external factors; (2) the number of equivalent polar directions is higher in the morphotropic region: 6 of [001] in the tetragonal structure, 8 [111] in the rhombohedral structure, and total of 14 in the morphotropic region. Similar

morphotropic R3m→P4mm phase transitions as well have been observed in other two-component systems, e.g., PMNT [2–3], PSNT [4–6] a.o. However, there are few studies of the morphotropic phase transition between Bmm2 (orthorhombic symmetry with a pseudomonoclinic unit cell) and P4mm structures. Such a phase transition might be of certain interest because of the 12 equivalent polar directions of the orthorhombic phase. For this reason ceramics of such a structure have the largest calculated value of polarization—0.912 of that of the relevant single crystal³⁰. Thus, the ferroelectric solid solutions having a tetragonal-monoclinic MPB are expected to possess good piezoelectric parameters. Possible coexistence of the structures is suggested by the P4mm→Bmm2 transition in BaTiO₃ where both the phases are observed in a certain interval of temperature [21].

The above considerations taken into account, the solid solution system $(1-x)\text{Pb}(\text{Lu}_{1/2}\text{Nb}_{1/2})\text{O}_3-x\text{PbTiO}_3$ was examined to investigate the structural, dielectric and piezoelectric properties of the ceramics, especially in the MPB region, in order to obtain a precise phase diagram.

2. Experimental

The compositions of the binary system PLuNT were synthesized with 10 mol% intervals of the PT concentration and with 1 mol% intervals near the MPB. According to X-ray data the MPB of the PLuNT powder is within the $(1-X)/X$ interval of 49/51–59/41. Refined X-ray data of ceramics yielded the morphotropic region with $\text{psd-M:T} \cong 1$ concentration within the 60/40–58/42 interval.

All the compositions of PLuNT ceramics were obtained by solid phase reactions from oxides according to the wolframite precursor method. The flow diagram outlining the preparation and testing steps are shown in Fig.1.

Silicon carbide (SiC) pistons and molds were used for hot-pressing and Al₂O₃ powder for package. The inside diameter of the mold was 30 mm. The hot-pressing was performed in two stages to find the best regime, the sample density being determined after each stage. The compositions vary over a wide range, and hot-pressing parameters have not been completely optimized at present.

Crystallographic studies were made by X-ray

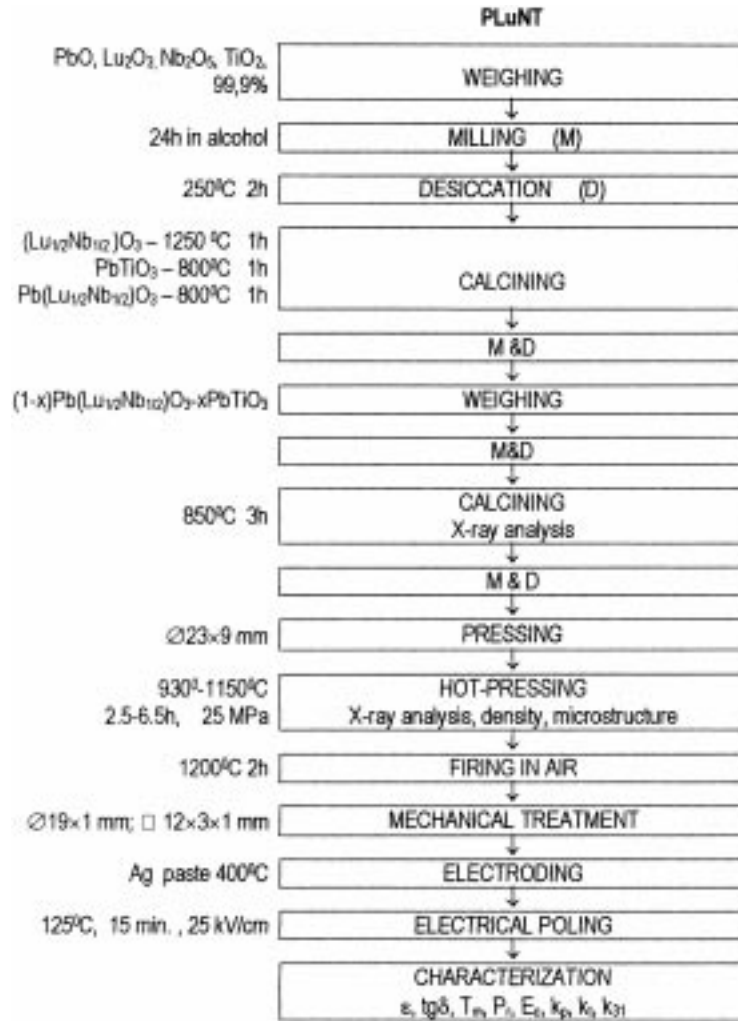


Fig. 1. Flow chart of the preparation and testing of PLuNT ceramics.

diffraction maxima 200, 220, 222 analysis using a DRON-UM1 diffractometer with Co K_{α} radiation, and Fe β filter. Linear and angular unit cell parameters were calculated from the relevant $1/d^2$ quadratic forms of the tetragonal and pseudomonoclinic cells by separating the phase components from the complex diffraction line profiles.

Density was determined by immersion after each stage of hot-pressing. To study the dielectric permittivity ϵ as function of the annealing temperature, the samples were heat treated for 2 h at

temperatures 1000–1200°C. Capacitance and dielectric loss were measured using a HP4284 LCR instrument; the dielectric hysteresis loops were obtained by the Sawyer-Tower circuit in quasistatic regime.

The piezoelectric measurements were made on samples poled for 15 min at 25 kV/cm and 125°C and cooled under field to room temperature. A HP4194 impedance analyzer was used to determine the piezoelectric characteristics by the IEEE resonance method [23].

3. Results and Discussion

3.1. Ceramic Properties

The hot-pressing temperature was different for different compositions: 950°C to 1100°C ($x < 0.2$ and $x > 0.7$) and 930–1050°C within the interval $0.2 < x < 0.7$. Because the molds were not hermetic, intense evaporation of PbO was observed during the hot pressing even at low hot-pressing temperatures. To compensate the loss, 1 wt % of excess PbO was used. However, this turned out not to be the optimum amount, being specific to each of the compositions, since excess PbO was found in particular samples after hot-pressing as well. Some PbO volatilized at final firing the hot-pressed ceramics in air (at 1200°C, 2 h) used to decrease the over-stoichiometric amount of lead oxide (Fig. 1).

The remaining PbO, on the other side, was responsible for poor polarization (leaky hysteresis loops) and lower electromechanical coupling. Polarization and piezoelectric properties of the PLuNT samples measured during the last step of the working program display this unwanted effect. Specific resistance of the PLuNT samples at room temperature is $3 \cdot 10^8 - 10^9 \Omega \cdot \text{m}$. At poling temperatures of 120–130 °C, it decreases to $10^7 \Omega \cdot \text{m}$.

Ceramic samples of PLuNT obtained from compositions with 1 wt % of excess PbO have a dense structure and comparatively large grains of the average size of 5–6 μm (Fig. 2a) while many small pores and average size of grains 1–2 μm and lower density are characteristic to samples from stoichiometric compositions (Fig. 2b).

Dependence of the hot-pressing temperature and density ρ of the PLuNT compositions on the mole concentration x of lead titanate (PT) is shown in Fig. 3. The density ρ gradually decreases if PT concentration increases as expected from the density values calculated from X-ray data: for “end” compositions PLuN and PT $\rho_{\text{calculated}}$ is 9.1 g/cm³ and 7.9 g/cm³, correspondingly.

The obtained results suggest that the PLuNT ceramics are sensitive to hot-pressing parameters (T, p, t) a strong control of which is required. If the temperature shifts even slightly from its optimal value, the density of the ceramics is too low and becomes inhomogeneous over the bulk of the sample, or decomposition of the ceramics occurs (around the

MPB the PLuNT decomposes at temperatures exceeding 1120°C).

In case of the PLuNT system, hot-pressing is made at a comparatively low temperature. Heat treatment temperature after hot-pressing can neither be high because of a rather low melting point.

3.2. Phase Diagram

According to X-ray diffraction data, all the obtained powders are nearly fully perovskite and the ceramic compounds are single-phase perovskites except for pure $\text{Pb}(\text{Lu}_{1/2}\text{Nb}_{1/2})\text{O}_3$ ceramics which, under the conditions of production, contained about 4 vol % of the pyrochlore phase (Table 1).

The following features of the phase diagram of the $(1-x)\text{Pb}(\text{Lu}_{1/2}\text{Nb}_{1/2})\text{O}_3 - x\text{PbTiO}_3$ solid solution system can be revealed (Fig. 4).

Pure lutecium niobate (PLuN) has a pronounced long-range order in the B sublattice (the X-ray diffraction pattern suggests a superstructure) and a pseudomonoclinic (psd-M) cell with linear parameters $a = c = 4.150 \text{ \AA}$, $b = 4.119 \text{ \AA}$ and an angle $\beta = 90.43^\circ$ (Fig. 4, Table 1); The space group of PLuN and compositions at small x is Bmm2 and the true unit cell is orthorhombic. A pseudomonoclinic primitive cell was used to analyze the X-ray diffraction data and to calculate parameter values. The orthorhombic ($a_{\text{orth}}, b_{\text{orth}}, c_{\text{orth}}$) and pseudomonoclinic (a, b, β) sets of parameters are associated by relations: $a_{\text{orth}} = 2a \sin \beta/2$; $b_{\text{orth}} = 2a \cos \beta/2$; $c_{\text{orth}} = b$.

With the increase of x (the concentration of PbTiO_3) the long-range order in the B sublattice disappears—the I_{111}/I_{200} ratio gradually changes from 0.919 to 0.054 as x is changed from 0 to 0.3 (Table 1). An intermediate phase between the antiferroelectric PLuN and ferroelectric PT is expected as in the case of PZ-PT system at small concentrations of PT ($x \geq 0.1$). This was not studied in detail in the present work. Piezoelectric coupling observed in compositions at $x \geq 0.3$ indicates the presence of the pseudomonoclinic ferroelectric phase.

With the growth of the content of PbTiO_3 , the angle β proceeds through a minimum in the pseudomonoclinic part of the phase diagram. At $x = 0.2$ the structure becomes pseudocubic, the angle β differs from 90° within the accuracy of measurement $\pm 0.02^\circ$ (Fig. 4a, inset, the corresponding broadening of X-ray diffraction maxima 222 being at the limit of experimental resolution).

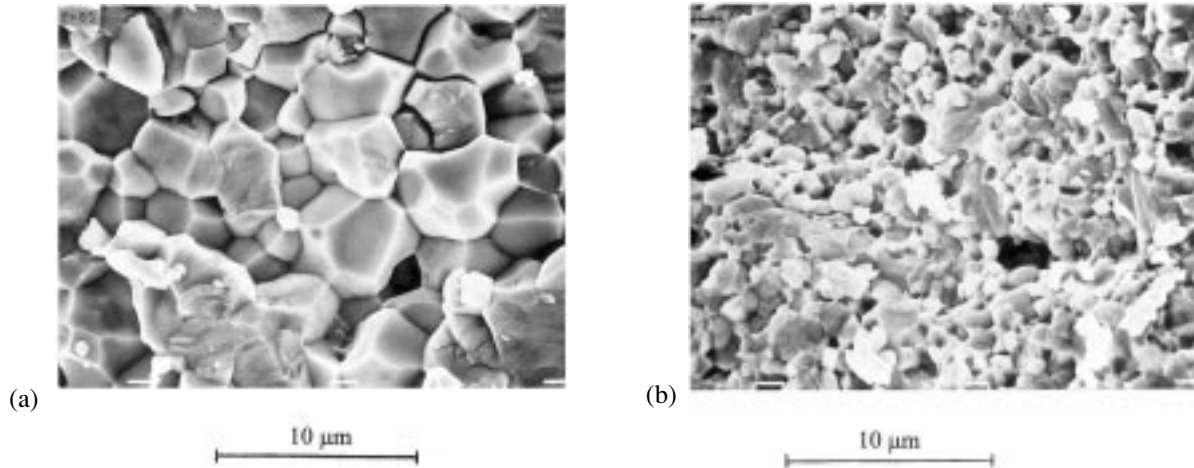


Fig. 2. SEM micrographs of the hot-pressed PLuNT ceramics: (a) PLuNT 58/42 + 1 wt % PbO; (b) PLuNT 59/41 synthesized without excess PbO.

The morphotropic region (detected by appearance of the diffraction component of the relevant phase in the complex 200 profile) extends over the concentration interval $x = 0.38\text{--}0.49$ (Fig. 4). The morphotropic phase boundary (MPB) with the concentration ratio $\text{psd-M:T} \cong 1$ corresponds to $x = 0.41$. Within the MPB interval, compared to the PZT system, a rather strong distortion of the unit cell ($c/a - 1 \geq 0.02$, $\beta \geq 90.37^\circ$) is maintained (Fig. 4). For this reason the pure PLuNT is a “hard” piezoelectric. Position of the MPB changes by 1–2 mol % depending on the amount of over-stoichiometric PbO in the synthesized PLuNT compound. E.g., if PbO is decreased from 1 wt % to zero, concentration x corresponding to equal amounts of

pseudomonoclinic and tetragonal phases changes from 0.41 (at 1 wt % of PbO) to 0.39 (at 0 wt % PbO).

Within the morphotropic region X-ray diffraction maxima are broader than compared to the rest of PT concentrations—the halfwidth of the 200 component is 0.5° (2θ scale). Outside the morphotropic region, its halfwidth reduces to 0.3° . This kind of effect is usually related to microtensions and/or dispersity. In the morphotropic region both of the effects are expected, the increase of dispersity in this case means that within a grain of ceramics (the size of which is practically constant over the whole interval) there are regions of coherent scattering centers of different symmetry.

The relative amount of phases within the MPB was determined from X-ray diffraction intensities normalized to compositional change of the structure factor with account for amount of the relevant phase and unit cell symmetry. The accuracy of 10–15% in this case, however, suggests that the so-called “lever rule”—the linear dependence on the concentration of one of the components, e.g., PbTiO_3 does not hold in the morphotropic region (Fig. 5). For that reason the morphotropic region is asymmetric with respect to the equal concentration of pseudomonoclinic and tetragonal phases. If the “lever rule” holds, this concentration corresponds to the middle point of the morphotropic region. In case of the PLuNT, the relevant concentration is displaced to the side of PLuN component, suggesting that the crystallographic structure of the tetragonal phase within a

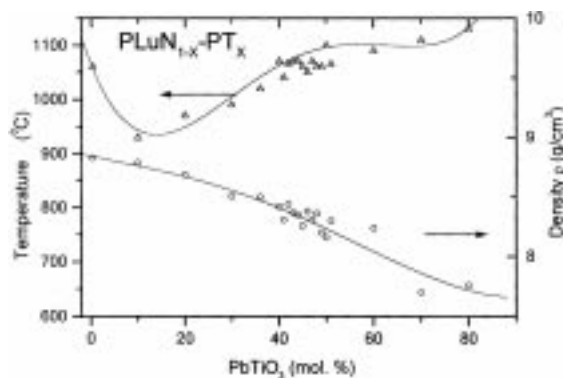


Fig. 3. Hot-pressing temperature and density of $\text{PLuN}_{1-x}\text{PT}_x$ ceramics vs. concentration of lead titanate.

Table 1. Physical and structural characteristics in PLuNT (1 - X)/X ceramics at various contents of lead titanate (mol %)

PbTiO ₃ (mol %)	0	10	20	30	36	40	41	50	60	70	80
Perovskite ratio	96	100	100	100	100	100	100	100	100	100	100
ρ	8.80	8.79	8.69	8.51	8.50	8.42	8.44	8.16	8.24	7.68	7.76
T_m	258	100	129	265	316	357	353	436	448	495	494
ϵ_{20}	126	750	2238	1429	—	1936	1228	713	477	723	198
$tg\delta$	0.012	0.047	0.070	0.054	—	0.043	0.044	0.011	0.022	0.02	0.03
ϵ_{max}	580	3896	7311	17,135	17,633	11,800	25,376	26,500	8607	6100	21,500
ϵ_{20} (pol.)	119	590	1990	814	907	1005	1083	—	477	—	—
k_p	—	—	—	0.39	—	0.52	0.66	—	0.20	—	—
k_t	—	—	—	0.41	—	0.42	0.48	—	—	—	—
k_{31}	—	—	—	0.21	0.27	0.28	0.36	—	—	—	—
Phase	psd-M	psd-M	psd-M	psd-M	psd-M	psd-M + T	MPB	T	T	T	T
I_{111}/I_{200}	0.919	0.545	0.299	0.054	0	0	0	0	0	0	0

Perovskite ratio—perovskite ratio of fired sample (%); ρ —density (g/cm^3); T_m —dielectric permittivity maximum temperature ($^{\circ}\text{C}$); ϵ_{20} , $\epsilon_{20}(\text{pol.})$, ϵ_{max} —dielectric permittivity at room temperature for unpoled and poled sample and maximum dielectric permittivity respectively; $tg\delta_{20}$ —dielectric loss at room temperature ($f = 1 \text{ kHz}$); k_p , k_t , k_{31} —electromechanical coupling factors for planar, thickness and transverse mode, respectively; psd-M—pseudomonoclinic; T—tetragonal, MPB—morphotropic phase boundary; I_{111}/I_{200} —X-ray diffraction maxima ratio (superstructure).

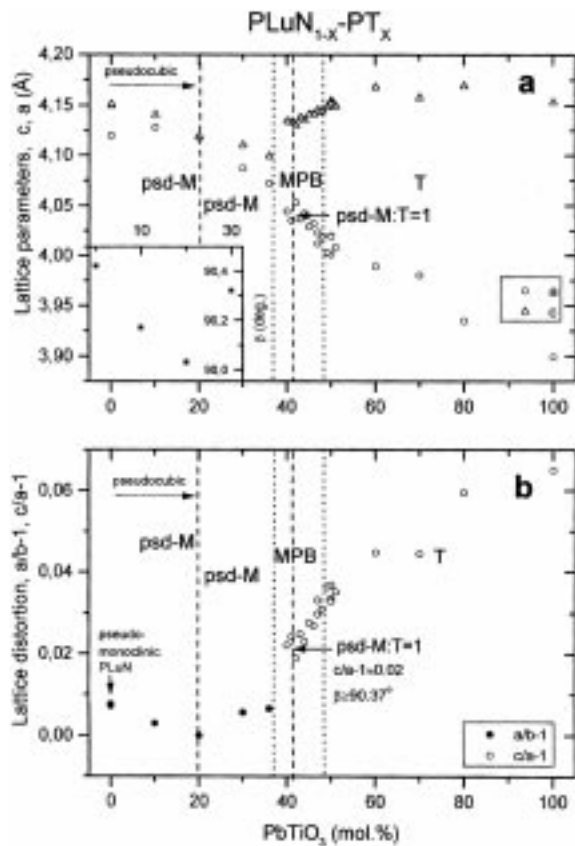


Fig. 4. The phase diagram of the PLuN_{1-x}PT_x system at room temperature: lattice parameters (a) and distortion of the unit cell (b) vs. concentration of PbTiO₃ (mol %). Inset (a)—concentration dependence of the monoclinic angle β .

pseudomonoclinic matrix is of higher stability compared to a pseudomonoclinic formation in a tetragonal matrix.

3.3. Dielectric Properties

The thermal dependence of the dielectric permittivity ϵ of (1-x) PLuN-xPT ceramics with different concentration x of lead titanate is shown in Figs. 6 and 7. An antiferroelectric-paraelectric (AFE-PE) phase transition at $\sim 258^{\circ}\text{C}$ is observed in pure lutecium niobate ($\epsilon(T)$ data—Fig. 6, inset). Broadening of the phase transition and dielectric dispersion, characteristic features of ferroelectric

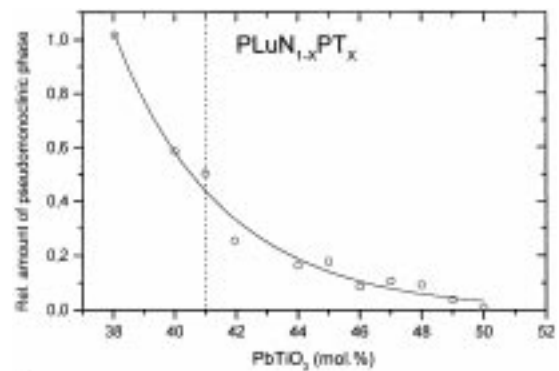


Fig. 5. Dependence of relative amount of monoclinic phase vs. PbTiO₃ content. $T = 20^{\circ}\text{C}$.

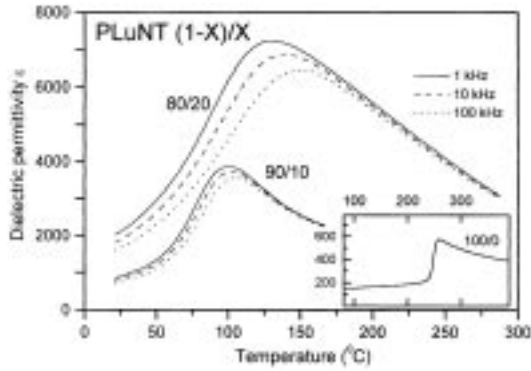


Fig. 6. Dielectric permittivity vs. temperature for PLuNT (1 - X)/X samples (X = 0; 10; 20 mol % PbTiO₃).

relaxors, e.g., PMN, PLZT are observed within the concentration interval of $0.1 \leq x \leq 0.3$ (Fig. 6). The peak values of ϵ increase with the increase of PT content and exceed 25,000 in the MPB region. However, it remains high (almost higher > 26,500) even at $x = 0.5$. Dependence of the dielectric permittivity maximum temperature T_m on concentration of PT is shown in Fig. 8. The lowest T_m is observed at $x = 0.1$, however near the MPB, $T_m > 350^\circ\text{C}$, which is the highest value among binary $\text{Pb}(\text{B}', \text{B}'')\text{O}_3$ -PT perovskites.

The minimum of the temperature function of the PT content corresponds to the lowest hot-pressing temperatures (Fig. 3). The dependence $T_m(x)$ in the case of PLuNT is very similar to that of PYbNT [11].

The dielectric hysteresis of PLuNT 59/41 as shown in Fig. 9 is characterized by rather high values of

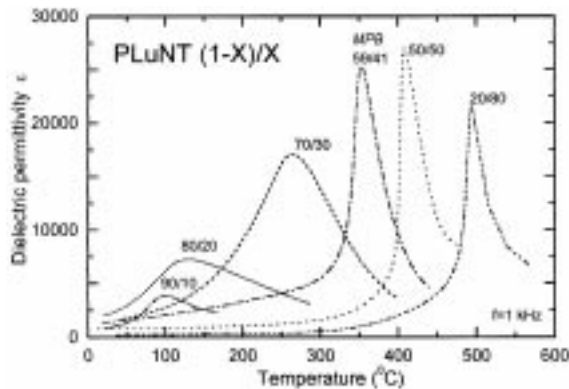


Fig. 7. Dielectric permittivity vs. temperature for PLuNT (1 - X)/X samples.

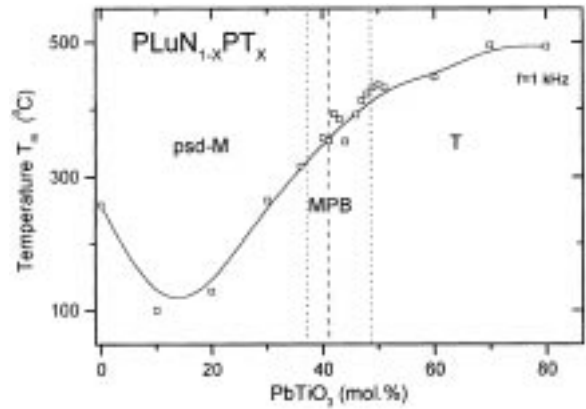


Fig. 8. Dielectric permittivity maximum ϵ_{max} temperature T_m vs. concentration of lead titanate X in $\text{PLuN}_{1-x}\text{PT}_x$ system.

coercive field $E_c = 22 \text{ kV/cm}$ and remanent polarization $P_r = 37 \mu\text{C/cm}^2$.

3.4. Piezoelectric Properties

Coefficients of electromechanical coupling (k_p —planar mode, k_t —thickness mode), as functions of the PT concentration x in the $(1-x)\text{PLuN}-x\text{PT}$ ceramic series, are shown in Fig. 10.

Both coefficients reach maxima at $x = 0.41$ (MPB compound): $k_p = 0.66$, $k_t = 0.48$. Compositions obtained from stoichiometric mixtures have much lower electromechanical coupling coefficients compared to those containing 1 wt % excess of PbO: $k_p = 0.54$, $k_t = 0.43$ at $x = 0.38$.

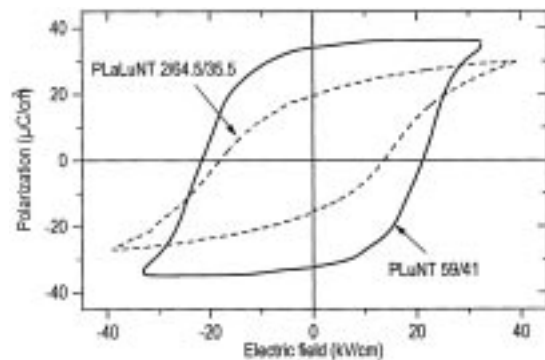


Fig. 9. Dielectric hysteresis loop for PLuNT 59/41 and PLuNT 2/64.5/35.5 ceramics.

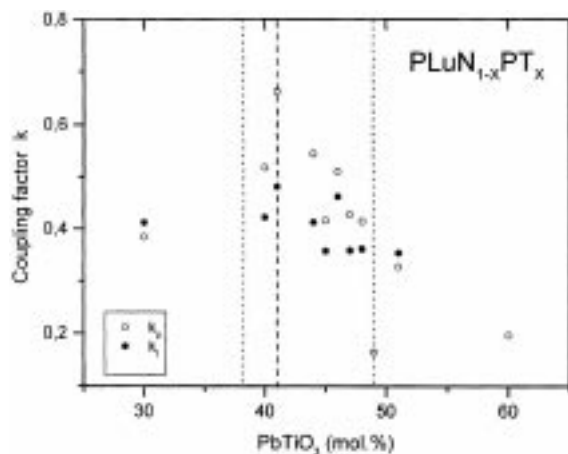


Fig. 10. The electromechanical coupling factors: planar— $k_p(a)$ and thickness— $k_t(b)$ for $\text{PLuN}_{1-x}\text{PT}_x$ ceramics in the MPB region.

The structural parameters and physical characteristics of the $(1-x)\text{PLuN}-x\text{PT}$ ceramics are summarized in Table 1.

The properties of PLuNT ceramics are sensitive to the change of technological parameters—respectively, dielectric and piezoelectric characteristics are expected to be essentially improved by particular optimization of calcining and hot-pressing regimes, additional heat treatment of the hot-pressed ceramics at high temperatures, by use of proper amount of excess PbO, by selection of optimal doping material and concentration.

3.5. Modification of PLuNT Ceramics

Substitution of $\text{La}^{3+} \rightarrow \text{Pb}^{2+}$ results in solid solutions limited to 15–20 at %. The mechanism compensating the imbalance of the electric charge at heterovalent substitution is: one vacancy in the Pb sublattice per two substituting atoms. Vacancies facilitate domain wall mobility and the switching process: the coercive field is reduced and poling is more efficient. All the effects are efficient, if defective solid solutions are formed. If an overstoichiometric modifier is introduced, a mechanism should exist providing place for it in the lattice.

Stoichiometric defective solid solutions provide a broader variety of possible concentration of modifiers and macroscopic properties of ceramics. In the case of heterovalent substitution of Pb^{2+} by La^{3+} according to $2\text{Pb}^{2+} \rightarrow 2\text{La}^{3+} + \text{A}$ (the corre-

sponding formula of PLuNT solid solutions is $(1-x)\text{Pb}_{1-1.5y}\text{La}_y\text{Lu}_{0.5}\text{Nb}_{0.5}\text{O}_3-x\text{Pb}_{1-1.5y}\text{La}_y\text{TiO}_3$, where $y = 0.01; 0.02$ is the molar concentration of La^{3+}), changes of the phase diagram near the morphotropic region are observed (Fig. 11).

The morphotropic phase boundary shifts towards PLuN (the concentration of the monoclinic phase corresponding to the MPB increases). The MPB of initial compositions corresponds to $x = 0.41$ while in case of modified compositions at $y = 0.01$ it corresponds to $x = 0.355$ and at $y = 0.02$ to $x = 0.35$. At the same time spontaneous deformation ($c/a-1$) of the unit cell decreases monotonously; outside region in the tetragonal part of the diagram $c/a-1$ diminishes at the rate 1.7×10^{-3} per 1 mol % of La^{3+} ; ($c/a-1$) corresponding to the MPB decreases to 0.015 at $y = 0.01$ and to 0.009 at $y = 0.02$, which means that modified composition are softer ferroelectrics compared to unmodified ones. The effect of La^{3+} on dielectric polarization is shown in Fig. 10. The relatively high values of induced and remanent polarization being maintained, the coercive field E_c of composition PLaLuNT 2/64.5/35.5 has decreased to 15.8 kV/cm. Coercive field is still further reduced to $E_c = 11$ kV/cm in PLaLuNT 2/65.5/34.5 which, regrettably, is accompanied by a decrease of the remanent polarization. The reason is the shift from morphotropic phase boundary (in case of composition PLaLuNT 2/65.5/34.5 the ratio psd-M:T $\approx 4:1$).

The effect of La-modifier on the dielectric and

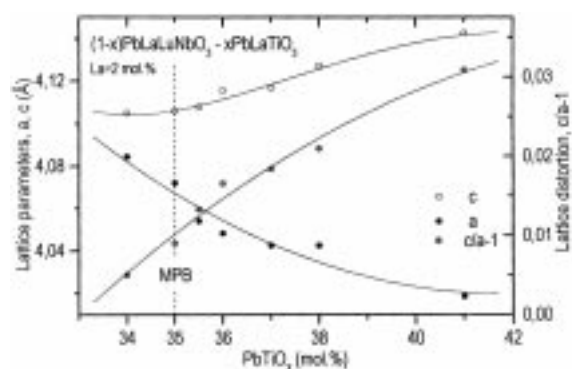


Fig. 11. The phase diagram of the lanthanum (2 mol %) modified PbLaLuNT system at room temperature: lattice parameters a and c , distortion of the unit cell $c/a-1$ vs. concentration of PbTiO_3 (mol %).

piezoelectric properties of the PLuNT system will be discussed in detail in a separate paper.

4. Conclusions

Solid solutions of the $(1-x)\text{Pb}(\text{Lu}_{1/2}\text{Nb}_{1/2})\text{O}_3-x\text{PbTiO}_3$ (PLuNT) binary system have been synthesized for the first time. Hot-pressed (temperature 930°C to 1130°C, pressure 25 MPa) ceramics have been obtained in the interval $0 < x < 0.80$ and the structural, dielectric and piezoelectric properties were investigated.

At room temperature, the phases change from pseudomonoclinic ($x < 0.38$) via pseudocubic at $x \approx 0.2$ to tetragonal ($x > 0.49$). Pure PLuN has a pronounced long-range order in the B sublattice (the X-ray diffraction contains superstructure maxima of a pseudo-pseudomonoclinic symmetry) and an antiferroelectric-paraelectric phase transition at $\sim 258^\circ\text{C}$. With the growth of the PbTiO_3 concentration, the angle β proceeds through a minimum in the pseudomonoclinic part of the phase diagram (at $x = 0.2$ the structure becomes pseudocubic, the angle β differs from 90° within the accuracy of measurement $\pm 0.02^\circ$). Dielectric dispersion and broadening of the phase transition—typical features of relaxors—are observed within the concentration interval of $0.1 \leq x \leq 0.3$. The morphotropic region extends over the interval $x = 0.38 - 0.49$, the concentration ratio $\text{psd-M:T} \cong 1$ corresponding to $x = 0.41$. Within this interval, compared to the PZT system, a rather strong distortion of the unit cell is maintained— $(c/a - 1) \geq 0.02$, $\beta \geq 90.37^\circ$ making the pure PLuNT a “hard” piezoelectric. Non-isovalent doping of PLuNT with La^{3+} in the Pb sublattice shifts the MPB to lower values of x , diminishes the distortion of the unit cell $c/a - 1 = 0.009$ at 2 mol % of La) and reduces the coercive field.

The maximum values of the electromechanical coupling coefficients $k_p = 0.66$, $k_t = 0.48$, $k_{31} = 0.36$ of $(1-x)\text{PLuN}-x\text{PT}$ ceramics are attained in compositions near the pseudomonoclinic/tetragonal MPB at $x = 0.41$.

The PLuNT system has strong electromechanical

coupling and among binary $\text{Pb}(\text{B}', \text{B}'')\text{O}_3$ -PT perovskites, the highest $T_m = 353^\circ\text{C}$. It may be a favorable material for piezoelectric sensors and actuators, utilized at high temperatures, and may be of interest for thin film and single crystal applications.

References

1. B. Jaffe, R.S. Roth, and S. Marzullo, *J. Res. Natl. Bur. Standard*, **55**, 239 (1955).
2. Q.M. Zhang, J. Zhao, and L.E. Cross, *J. Appl. Phys.*, **79**(6), 3181 (1996).
3. O. Noblanc, P. Gaucher, and G. Calvarin, *J. Appl. Phys.*, **79**(8), 4291 (1996).
4. Y. Yamashita, *Jpn. J. Appl. Phys.*, **32**, 5036 (1993).
5. Y. Yamashita, *Jpn. J. Appl. Phys.*, **33**, 5328 (1994).
6. A. Kalvane, M. Antonova, M. Livinsh, M. Kundzinsh, A. Spule, L. Shebanovs, and A. Sternberg, *Key Engineering Materials*, **132–136**, 1072 (1997).
7. J.R. Giniewitz, A.S. Bhalla, and L.E. Cross, *Ferroelectrics*, **211**, 281 (1998).
8. Y. Yamashita, K. Harada, T. Tao, and N. Ichinose, *Integrated Ferroelectrics*, **13**, 9 (1996).
9. M. Dambekalne, I. Brante, M. Antonova, and A. Sternberg, *Ferroelectrics*, **131**, 67 (1992).
10. H. Zhu, Y. Tan, Q. Wang, Z. Cai, and Z. Meng, *Jpn. J. Appl. Phys.*, **33**, 6623 (1994).
11. T. Yamamoto and S. Ohashi, *Jpn. J. Appl. Phys.*, **34**, 5349 (1994).
12. E.F. Alberta and A.S. Bhalla, *J. of the Korean Phys. Soc.*, **32**, S1265 (1998).
13. M. Kondo, M. Hida, M. Tsukada, K. Kurihara, and N. Kamehara, *Jpn. J. Appl. Phys.*, **36**, 6043 (1997).
14. T. Yamamoto and Y. Yamashita, in *Proc. ISAF'96* (East Brunswick, NJ, U.S.A., **2**, 1996), p. 573.
15. Tai-Bor Wu, Ming-Jyx Shyu, Chia-Chi Chung, and Hsin-Yi Lee, *J. Am. Ceram. Soc.*, **78**(8), 2168 (1995).
16. J. Zhao, Q.M. Zhang, N. Kim, and T. Shrout, *Jpn. J. Appl. Phys.*, **34**, 5658 (1995).
17. J. Kuwata, K. Uchino, and S. Nomura, *Jpn. J. Appl. Phys.*, **21**, 1298 (1982).
18. S. Shimanuki, S. Saito, and Y. Yamashita, *Jpn. J. Appl. Phys.*, **37**, 3382 (1998).
19. S.E. Park and T.R. Shrout, *J. Appl. Phys.*, **82**(4), 1804 (1997).
20. T. Shrout, Z.P. Zhang, N. Kim, and S. Markgraf, *Ferroelectric Letters*, **12**, 63 (1990).
21. H.G. Baerwald, *Phys. Rev.*, **105**, 480 (1957).
22. L.A. Shebanovs, *phys .stat. sol.(a)*, **65**, 321 (1981).
23. IEC Standard Publication 483, *Guide to Dynamic Measurements of Piezoelectric Ceramics with High Electromechanical Coupling* (1976).